

# Comparison of Four Bifunctional Chelates for Radiolabeling Monoclonal Antibodies with Copper Radioisotopes: Biodistribution and Metabolism

Buck E. Rogers,<sup>†,‡</sup> Carolyn J. Anderson,<sup>\*,†</sup> Judith M. Connett,<sup>‡</sup> Li Wu Guo,<sup>‡</sup> W. Barry Edwards,<sup>†</sup> Elizabeth L. C. Sherman,<sup>†</sup> Kurt R. Zinn,<sup>§,¶</sup> and Michael J. Welch<sup>†</sup>

The Edward Mallinckrodt Institute of Radiology and Department of Surgery, Washington University School of Medicine, St. Louis, Missouri 63110, and University of Missouri Research Reactor, Columbia, Missouri 65211. Received March 22, 1996<sup>⊗</sup>

The bifunctional chelating agents (BFCs), 6-[*p*-(bromoacetamido)benzyl]-1,4,8,11-tetraazacyclotetradecane-1,4,8,11-tetraacetic acid (BAT), 6-[*p*-(isothiocyanato)benzyl]-1,4,8,11-tetraazacyclotetradecane-1,4,8,11-tetraacetic acid (SCN-TETA), 4-[(1,4,8,11-tetraazacyclotetradec-1-yl)methyl]benzoic acid (CPTA), and 1-[(1,4,7,10,13-pentaazacyclopentadec-1-yl)methyl]benzoic acid (PCBA), were synthesized and conjugated to the anti-colorectal monoclonal antibody (mAb), 1A3, and antibody fragments, 1A3-F(ab')<sub>2</sub>, for radiolabeling with <sup>64,67</sup>Cu and comparison in animal models. *In vivo* metabolism studies were carried out in liver and kidneys in order to correlate the nature of the metabolites formed to the uptake and retention of the radiolabel in each organ. Animal biodistribution studies were performed in Golden Syrian hamsters bearing the GW39 human colon cancer tumors and in normal Sprague–Dawley rats. All conjugates showed good tumor uptake in hamsters. Biodistribution in rats showed that <sup>64</sup>Cu-BAT-2IT-1A3 had the lowest liver and kidney uptake of the intact 1A3 conjugates (*p* < 0.03), whereas in hamsters, there were no significant differences in liver and kidney uptake between the four intact BFC-1A3 conjugates. Tumor-bearing hamsters injected with <sup>64</sup>Cu-CPTA-1A3-F(ab')<sub>2</sub> and <sup>64</sup>Cu-PCBA-1A3-F(ab')<sub>2</sub> had from 3 to 7 times greater uptake in the kidneys than hamsters given <sup>64</sup>Cu-labeled BAT and SCN-TETA 1A3-F(ab')<sub>2</sub> conjugates, while rats injected with <sup>64</sup>Cu-CPTA-1A3-F(ab')<sub>2</sub> and <sup>64</sup>Cu-PCBA-1A3-F(ab')<sub>2</sub> had nearly twice the uptake. The *in vivo* metabolism of the mAbs 1A3 and 1A3-F(ab')<sub>2</sub> radiolabeled with <sup>67</sup>Cu through the SCN-TETA, CPTA, and PCBA BFCs was investigated by excising the livers and kidneys of normal rats from 1–5 days post-injection of the radiolabeled conjugates. Liver and kidney homogenates were analyzed by size exclusion chromatography and thin layer chromatography (TLC). The size exclusion chromatography data showed that all of the <sup>67</sup>Cu-labeled 1A3-F(ab')<sub>2</sub> conjugates were >85% degraded in the kidneys to small molecular weight metabolites by 1 day post-injection. In contrast, in the liver at 1 day post-injection, greater than 70% of the <sup>67</sup>Cu-labeled 1A3 conjugates were unmetabolized. By day 5, a 35 kDa peak appeared in the liver of rats injected with the <sup>67</sup>Cu-labeled 1A3 conjugates, possibly due to transchelation of the <sup>67</sup>Cu to proteins. Superoxide dismutase chromatographically elutes at the same retention time as this <sup>67</sup>Cu-labeled metabolite. The TLC data indicate that the low molecular weight metabolite (<5 kDa) of both <sup>67</sup>Cu-CPTA-1A3 and <sup>67</sup>Cu-CPTA-1A3-F(ab')<sub>2</sub> conjugates co-chromatographed with a <sup>67</sup>Cu-CPTA- $\epsilon$ -lysine standard. Our data suggest that chelate charge and lipophilicity play a large role in kidney retention of <sup>64/67</sup>Cu-labeled BFC-1A3-F(ab')<sub>2</sub> conjugates, while transchelation of the copper label appears to be the major factor for liver accumulation of <sup>64/67</sup>Cu-labeled BFC-1A3 conjugates.

## INTRODUCTION

The specificity of mAbs<sup>1</sup> for their antigens has led to their use in targeting cancer cells. Radiolabeled mAbs have been used for the early detection and therapy of cancer (1, 2). Monoclonal antibodies labeled with copper isotopes have applications in both diagnosis and therapy. <sup>67</sup>Cu emits abundant  $\beta^-$  (100%) with the subsequent emission of  $\gamma$  photons for both therapeutic and imaging applications (3–5), while <sup>64</sup>Cu decays by  $\beta^+$  and  $\beta^-$  which

also allows its use in both PET imaging (6–8) and radiotherapy (9–11).

It has been demonstrated that the BFC used to complex radiometals to mAbs has a significant effect on the biodistribution in animal models (12–15). The purpose of this study was to gain a better understanding of how the nature of the BFC affects biodistribution of Cu-labeled mAbs. Four BFCs (BAT, SCN-TETA, CPTA, and PCBA (Figure 1)) that differ in charge, lipophilicity, and covalent linkage to the mAb were synthesized and

\* Address correspondence to Carolyn J. Anderson, Ph.D., Mallinckrodt Institute of Radiology, Washington University School of Medicine, 510 S. Kingshighway Blvd Box 8225, St. Louis, MO 63110. Phone: (314) 362-8435. FAX: (314) 362-9940. e-mail: andersoncj@mirlink.wustl.edu.

<sup>†</sup> Edward Mallinckrodt Institute of Radiology.

<sup>‡</sup> Department of Surgery.

<sup>§</sup> University of Missouri Research Reactor.

<sup>¶</sup> Present Address: The University of Alabama at Birmingham, Birmingham, AL 35233.

<sup>⊗</sup> Abstract published in *Advance ACS Abstracts*, June 15, 1996.

<sup>1</sup> Abbreviations: mAb, monoclonal antibody; PET, positron emission tomography; BFC, bifunctional chelating agent; BAT, 6-[*p*-(bromoacetamido)benzyl]-1,4,8,11-tetraazacyclotetradecane-1,4,8,11-tetraacetic acid; SCN-TETA, 6-[*p*-(isothiocyanato)benzyl]-1,4,8,11-tetraazacyclotetradecane-1,4,8,11-tetraacetic acid; CPTA, 4-[(1,4,8,11-tetraazacyclotetradec-1-yl)methyl]benzoic acid; PCBA 1-[(1,4,7,10,13-pentaazacyclopentadecyl-1-yl)methyl]benzoic acid; 2IT, 2-iminothiolane; FPLC, fast protein liquid chromatography; EDC, 1-ethyl-3-[3-(dimethylamino)propyl]carbodiimide; sNHS, *N*-hydroxysulfosuccinimide; IR, immunoreactivity; SOD, superoxide dismutase; Fmoc, fluorenylmethoxycarbonyl; boc, butoxycarbonyl; HOBt, hydroxybenzotriazole.

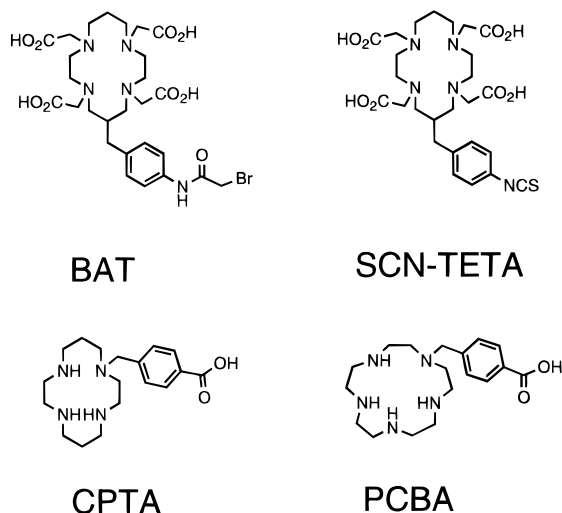


**Figure 1.** Structures of the bifunctional chelating agents used for labeling  $^{64,67}\text{Cu}$  to mAb 1A3 and 1A3-F(ab')<sub>2</sub>.

conjugated to intact mAb and mAb-F(ab')<sub>2</sub> and labeled with  $^{64}\text{Cu}$  or  $^{67}\text{Cu}$ . The biodistribution in two animal models and *in vivo* metabolism by normal rats of  $^{64,67}\text{Cu}$ -labeled BFC-mAb conjugates are compared.

The four BFCs were conjugated to the anti-colorectal mAb 1A3 and 1A3-F(ab')<sub>2</sub> fragments. This antibody has been previously conjugated with BAT, labeled with  $^{64}\text{Cu}$ , and evaluated in tumor-bearing hamsters and normal rats (16, 17). Tumor uptake for  $^{64}\text{Cu}$ -BAT-2IT-1A3 and  $^{64}\text{Cu}$ -BAT-2IT-1A3-F(ab')<sub>2</sub> was shown to be superior to both the  $^{111}\text{In}$ - and  $^{125}\text{I}$ -labeled 1A3 and 1A3-F(ab')<sub>2</sub> (16), and both  $^{64}\text{Cu}$  agents have been investigated clinically as PET imaging agents for colorectal cancer (6–8). One drawback of  $^{64}\text{Cu}$ -BAT-2IT-1A3-F(ab')<sub>2</sub> was the high accumulation in the kidneys of both animal models (17) and humans (7). Since the nature of the BFC appears to play an important role in the biodistribution of metal-labeled BFC-mAb conjugates, in the present study, we compare the *in vivo* behavior of  $^{64}\text{Cu}$ -labeled mAbs conjugated with the BFCs SCN-TETA, CPTA, PCBA, and BAT.

The BFCs are primarily conjugated to the mAbs through the  $\epsilon$ -amino of lysines (18), although conjugation to other amino acids bearing a nucleophilic side chain or the N-terminus cannot be excluded. The bifunctional chelate SCN-TETA was chosen to compare to BAT because the only difference in structure between the two BFCs is the covalent linkage to the mAbs. SCN-TETA forms a thiourea bond when linked to primary amines, while BAT is conjugated to mAbs using the linking agent 2IT which forms a thioether bond between BAT and the mAb (19). The Cu(II) complexes of BAT and SCN-TETA bear a net formal charge of 2–.

The CPTA and PCBA BFCs both form Cu(II) complexes with a net charge of 2+, and they are conjugated to mAbs via an amide linkage. The CPTA BFC has been used by Smith-Jones and co-workers in labeling  $^{67}\text{Cu}$  to AB35, a mAb directed against carcinoembryonic antigen (CEA) (20). This radioimmunoconjugate was evaluated in tumor-bearing mice and showed high tumor uptake (20). CPTA is readily synthesized in a one-step reaction and forms a stable complex with copper *in vivo* (20). PCBA is a BFC which is similar in structure to CPTA and can also be synthesized in a single step. The macrocyclic portion of PCBA is 15aneN5 which forms a stable complex with Cu(II) ( $\log K = 26.73$ ) (21). The stability constant of Cu(II)-15aneN5 is similar to that of Cu(II)-cyclam ( $\log K = 28.09$ ) (21) and greater than the stability

constant of Cu(II)-TETA (the macrocyclic chelate portion of the BFCs BAT and SCN-TETA) ( $\log K = 21.87$ ) (22). The similarity in complex stability of Cu(II)-15aneN5 to Cu(II)-cyclam and the fact that the 15aneN5 macrocycle is less lipophilic than cyclam made PCBA an interesting chelate for comparative purposes.

Metabolism studies on  $^{111}\text{In}$ -labeled antibodies and polypeptides have been conducted to gain a better understanding of the mechanisms involved in the uptake and retention of activity in nontarget organs (i.e., liver and kidneys) (23–30). We previously identified  $^{111}\text{In}$ -DTPA- $\epsilon$ -lysine as the major small molecular weight metabolic product of  $^{111}\text{In}$ -labeled 1A3 and 1A3-F(ab')<sub>2</sub> conjugates in the livers and kidneys of normal rats (30). In the present study, we compared the liver and kidney metabolism of  $^{67}\text{Cu}$ -labeled SCN-TETA, CPTA, and PCBA conjugates of 1A3 and 1A3-F(ab')<sub>2</sub> in normal rats to correlate the nature of the metabolites with the accumulation of radioactivity in nontarget organs (30).

## MATERIALS AND METHODS

1-Ethyl-3-[3-(dimethylamino)propyl]carbodiimide-HCl (EDC) and *N*-hydroxysulfosuccinimide (sNHS) were purchased from Pierce Chemical Co. (Rockford, IL). Centricon 30 concentrators were purchased from Amicon Inc. (Beverly, MA). Bio-Spin 6 chromatography columns were from Bio-Rad Laboratories (Hercules, CA). Sephadex G-25/50, diisopropylcarbodiimide (DIC), and superoxide dismutase (SOD) were purchased from Sigma Chemical Co. (St. Louis, MO).  $\epsilon$ -Fmoc- $\alpha$ -Boc-lysine and *p*-(benzyloxy)benzyl alcohol resin were purchased from NovaBiochem (LaJolla, CA). Ultrapure ammonium dihydrogen phosphate ( $\text{NH}_4\text{H}_2\text{PO}_4$ ) was purchased from Johnson Matthey (Royston, England). Ultrapure (>99%) ammonium acetate ( $\text{NH}_4\text{OAc}$ ) and ammonium citrate ( $\text{NH}_4\text{Cit}$ ) were purchased from Fluka (Ronkonkoma, NY). Disodium hydrogen phosphate ( $\text{Na}_2\text{HPO}_4$ ) and 4-(dimethylamino)pyridine (DMAP) were purchased from Fisher Chemical Co. (Fair Lawn, NJ). All other chemicals used were purchased from Aldrich Chemical Co. (Milwaukee, WI). All solutions were made using distilled deionized water (Milli-Q;  $\sim 18\text{ M}\Omega$  resistivity). Bio-Spin and Sephadex G-25/50 columns were equilibrated with 0.1 M  $\text{NH}_4\text{OAc}$  (pH 5.5) prior to use. The mAbs 1A3 and 1A3-F(ab')<sub>2</sub> were purified from serum-free medium by Invitron (St. Louis, MO) using proprietary methods. Adult, female Sprague-Dawley rats were purchased from Sasco (Omaha, NE), and Golden Syrian hamsters were purchased from Charles River (Wilmington, MA). A Tekmar tissue homogenizer (Cincinnati, OH), a Branson Sonifier 185 cell disrupter, and a Sorvall RC2-B centrifuge were used in the metabolism experiments. A Pharmacia Superose 12 gel filtration column was used in conjunction with a Pharmacia/LKB FPLC system (Piscataway, NJ) for metabolite analyses. A Beckman Gamma 8000 automated well type  $\gamma$  counter was used to count the FPLC fractions. Radio-TLC was carried out using a Bioscan System 200 Imaging Scanner.  $^{67}\text{Cu}$  (115.6–215.9 Ci/mmol) was purchased from Brookhaven National Laboratories.  $^{64}\text{Cu}$  (4572–15240 Ci/mmol) was produced and purified at the University of Missouri-Columbia Research Reactor as previously described (16, 31).

**Ligand Syntheses.** A method similar to Moi et al. and Moran et al. was used in the synthesis of nitrobenzyl-TETA, the direct precursor to BAT and SCN-TETA (32, 33). Briefly, the diethyl malonate anion was generated with NaH in THF and alkylated with *p*-nitrobenzyl bromide to give 2-(*p*-nitrobenzyl)diethyl malonate. The cyclic amide was formed under high dilution conditions

in EtOH from the diester and *N,N*-bis(2-aminoethyl)-1,3-diaminopropane. After refluxing for 8 weeks, the cyclic amide was isolated by slow evaporation of the solvent and subsequently reduced with  $\text{BH}_3\cdot\text{THF}$ . The cyclic amine was alkylated with 4 equiv of *tert*-butyl bromoacetate in acetonitrile (ACN) at room temperature. The reaction mixture was concentrated, and the *tert*-butyl groups were removed with trifluoroacetic acid. Nitrobenzyl-TETA was purified by anion exchange chromatography. Nitrobenzyl-TETA was then converted to BAT through a method described by McCall et al. (19) and converted to SCN-TETA through a method described by McMurry et al. (34).

CPTA was synthesized according to the method of Studer and Kaden (35), while PCBA was synthesized using a similar method described by Motekaitis et al. (21).

CPTA- $\epsilon$ -lysine was synthesized using a solid-phase procedure modeled after the previously described solid-phase synthesis of DTPA- $\epsilon$ -lysine (29). DIC (164  $\mu\text{L}$ , 1.05 mmol), HOBT (142 mg, 1.05 mmol), DMAP (12.8 mg, 0.105 mmol), and  $\epsilon$ -Fmoc- $\alpha$ -Boc-lysine (492 mg, 1.05 mmol) were added to 5.2 mL of DMF and stirred for 5 min at room temperature. To this was added 750 mg of the *p*-(benzyloxy)benzyl alcohol resin (hydroxyl substitution level of 0.7 mmol/g), and the mixture was stirred at room temperature overnight (~16 h). Then, the mixture was filtered and rinsed three times with 5 mL of DMF and three times with 10 mL of MeOH. The level of lysine substitution on the resin was determined using a UV absorbance test. DMF (100  $\mu\text{L}$ ) and piperidine (100  $\mu\text{L}$ ) were added to 1–2 mg of the substituted resin, and the mixture was incubated at room temperature for 30 min. After dilution with 4.8 mL of MeOH, the absorbance of fulvene was measured at  $\lambda = 301 \text{ nm}$  ( $\epsilon = 7800 \text{ M}^{-1} \text{ cm}^{-1}$ ). Triplicate measurements yielded an amino acid substitution level of 0.24 mmol/g. The  $\epsilon$ -Fmoc group was removed by stirring in 150 mL of 1:1 DMF:piperidine for 1 h at room temperature. The mixture was filtered, and the resin was rinsed with DMF followed with MeOH. CPTA (200 mg, 0.60 mmol), HOBT (80.9 mg, 0.60 mmol), and DIC (94.3  $\mu\text{L}$ , 0.60 mmol) were dissolved in 5 mL of DMF and added to the Fmoc-deprotected resin (625 mg, 0.15 mmol). After reaction overnight at room temperature, the mixture was filtered and the resin rinsed as above. The CPTA- $\epsilon$ -lysine was cleaved from the resin over a 75 min period using 2 mL of 95:5 trifluoroacetic acid (TFA):water, simultaneously removing the  $\alpha$ -Boc group. The mixture was filtered, concentrated, and diluted to 1.0 mL with  $\text{H}_2\text{O}/0.1\% \text{ TFA}$ .

A portion of the CPTA- $\epsilon$ -lysine was then purified by reversed-phase HPLC (Vydac 201HS1010,  $10 \times 250 \text{ mm}$ , C-18) with a 10 min isocratic elution at 10% A, followed by a linear gradient of 10% to 80% A over the next 10 min at 2.0 mL/min, where A = ACN/0.1% TFA and B =  $\text{H}_2\text{O}/0.1\% \text{ TFA}$ . Fractions were collected and analyzed by RP-HPLC at  $\lambda = 272 \text{ nm}$  using 2% A as the starting eluant and followed by a linear gradient of 10% to 80% A over 10 min. The desired product eluted at 21.3 min and was greater than 98% pure by RP-HPLC. The identity of the product was confirmed by electrospray MS  $m/e \text{ (M + H)}^+ = 463.65 \text{ g/mol}$ , calcd = 463.63 g/mol.

**Copper Challenge Experiments.**  $^{67}\text{Cu}$ -labeled TETA, CPTA, and PCBA were prepared by incubating the ligands in 0.1 M  $\text{NH}_4\text{OAc}$  (pH 5.5) with  $^{67}\text{Cu}$  acetate for 1 h at room temperature. A 10-fold molar excess of  $\text{CuCl}_2$  to ligand was added and the mixture allowed to incubate at room temperature. At various time points, 2  $\mu\text{L}$  of the  $^{67}\text{Cu}$ -TETA and  $^{67}\text{Cu}$ -CPTA solutions were applied to silica gel TLC plates and eluted using 1:1 MeOH:10%  $\text{NH}_4\text{OAc}$  in water. The silica plates were then dried and

analyzed with a radio-TLC scanner to determine the amount of copper complex that remained. At various time points, 100  $\mu\text{L}$  of the  $^{67}\text{Cu}$ -PCBA solution was passed through a 0.45  $\mu\text{m}$  Chelex chelating filter. Uncomplexed  $^{67}\text{Cu}$  bound to the filter, while  $^{67}\text{Cu}$ -PCBA passed through the filter.

**Conjugation of BAT, CPTA, PCBA, and SCN-TETA to 1A3 and 1A3-F(ab')<sub>2</sub>.** BAT was conjugated to 1A3 or 1A3-F(ab')<sub>2</sub> in 0.1 M  $\text{NH}_4\text{H}_2\text{PO}_4$  (pH 8). An aqueous solution of BAT was added to the buffered antibody in a 20:1 molar ratio (BAT:mAb) followed by the addition of 2IT in 50 mM triethanolamine hydrochloride in a 10:1 molar ratio (2IT:mAb). The solution was incubated at 37 °C for 30 min and purified using a Sephadex G-25/50 spin column (36) equilibrated in 0.1 M  $\text{NH}_4\text{Cit}$  (pH 5.5). BAT-2IT-1A3-F(ab')<sub>2</sub> was purified by FPLC as previously described (17). The conjugated mAbs were stored at -80 °C until needed (16).

CPTA was conjugated using an adaptation of the method described by Smith-Jones (20). CPTA (5.0 mg, 0.010 mmol), EDC (9.2 mg, 0.048 mmol), and sNHS (5.0 mg, 0.230 mmol) were dissolved in 359  $\mu\text{L}$  of 0.1 M  $\text{NH}_4\text{H}_2\text{PO}_4$  (pH 7.0) and incubated at room temperature. After 1 h, another 359  $\mu\text{L}$  of buffer was added and the solution was vortexed. A volume equal to a 50-fold molar excess of the ligand over antibody was added to the antibody (0.050 mM 1A3 and 0.065 mM 1A3-F(ab')<sub>2</sub>) at room temperature. The samples were incubated at room temperature for 2 h before they were purified by either a Bio-Spin or Sephadex G-25/50 spin column purification (36). Reaction volumes that were greater than 100  $\mu\text{L}$  and masses of greater than 1 mg of mAb were purified using a Sephadex column, while smaller volumes and amounts of mAb were purified using a Bio-Spin column. PCBA was conjugated to 1A3 or 1A3-F(ab')<sub>2</sub> similarly to CPTA mAbs as described above.

1A3 and 1A3-F(ab')<sub>2</sub> were concentrated using a Centricon 30 and then diluted with  $\text{Na}_2\text{HPO}_4$  (pH 10.5) prior to conjugation with SCN-TETA. The concentrated solutions were collected and diluted to give approximately 0.027 and 0.043 mM solutions for 1A3 and 1A3-F(ab')<sub>2</sub>, respectively. SCN-TETA was dissolved in  $\text{H}_2\text{O}$  to give a 1 mM solution. A volume equal to a 1.2 M excess of this solution was added to the antibody solutions, vortexed, and incubated at room temperature for 1 h. The conjugate was then added to a Centricon 30, diluted to 2.0 mL with 0.1 M  $\text{NH}_4\text{OAc}$  (pH 5.5), and centrifuged. This procedure was repeated and the conjugate collected from the membrane. Purities of all compounds were confirmed by FPLC. The BFC-mAb conjugates were stored at -80 °C until needed.

**Radiolabeling of BAT, SCN-TETA, CPTA, and PCBA-1A3 and 1A3-F(ab')<sub>2</sub> with  $^{64}\text{Cu}$  and  $^{67}\text{Cu}$ .**  $^{64}\text{CuCl}_2$  or  $^{67}\text{CuCl}_2$  in 0.1 M HCl was converted to  $^{64,67}\text{Cu}$  acetate by a 10-fold dilution with 0.1 M  $\text{NH}_4\text{OAc}$  (pH 5.5). The  $^{64,67}\text{Cu}$  acetate solution was then added to the desired chelate-antibody conjugate and incubated at room temperature for 30 min. The resulting radiolabeled conjugates were purified using Bio-Spin columns equilibrated with 0.1 M  $\text{NH}_4\text{OAc}$  (pH 5.5). The immunoreactivities of the resulting conjugates were determined as previously described (16).

**Radiolabeling of SOD with  $^{64}\text{Cu}$  and Analysis by FPLC.** SOD was labeled with  $^{64}\text{Cu}$  using the same method as described above for labeling mAbs. The resulting  $^{64}\text{Cu}$ -SOD was analyzed by FPLC.

**Golden Syrian Hamster and Sprague-Dawley Rat Biodistribution Studies.** All animal experiments were carried out according to guidelines specified by the

Washington University Animal Studies Committee and the Jewish Hospital Animal Care Committee.

Six week old male Golden Syrian hamsters (~100 g) were implanted with GW39 human colon carcinoma in the musculature of their right thigh 2 days prior to injection of the radiolabeled conjugates, as described previously (37). Hamster biodistribution experiments were carried out as previously described (16).

Adult, female Sprague–Dawley rats (~185 g) were intravenously injected with 25–50  $\mu\text{g}$  and 5–10  $\mu\text{Ci}$  of the  $^{64}\text{Cu}$ –antibody conjugates. For each compound, groups of at least three rats were sacrificed at 6, 12, and 24 h post-injection. Samples of blood, lung, liver, spleen, kidney, muscle, bone, ovaries, small intestine, upper large intestine, and lower large intestine were removed, weighed, and activity counted. The percent of injected dose per gram of tissue (%ID/g) and percent of injected dose per organ (%ID/organ) were calculated.

Blood clearance data were obtained from rats at 1, 3, 6, 12, and 24 h time points. Blood was drawn from the rats in ~100  $\mu\text{L}$  aliquots at the various time points, weighed, and counted to calculate the %ID/g.

**In Vivo Metabolism in Sprague–Dawley Rats.** Mature, female Sprague–Dawley rats were intravenously injected with 80–250  $\mu\text{Ci}$  of  $^{67}\text{Cu}$ -SCN-TETA-1A3 and  $^{67}\text{Cu}$ -SCN-TETA-1A3-F(ab')<sub>2</sub>, 100–400  $\mu\text{Ci}$  of  $^{67}\text{Cu}$ -PCBA-1A3 and  $^{67}\text{Cu}$ -PCBA-1A3-F(ab')<sub>2</sub>, or 400–1100  $\mu\text{Ci}$  of  $^{67}\text{Cu}$ -CPTA-1A3 and  $^{67}\text{Cu}$ -CPTA-1A3-F(ab')<sub>2</sub>. Livers were removed from rats injected with  $^{67}\text{Cu}$ -BFC-1A3 and kidneys were removed from rats injected with  $^{67}\text{Cu}$ -BFC-1A3-F(ab')<sub>2</sub> at 1, 3, and 5 day time points.  $^{67}\text{Cu}$  acetate was used as a control. The organs were rinsed with water to remove as much blood as possible, homogenized in labeling buffer using a Tekmar tissue homogenizer, and sonicated (3 min, power = 4). The samples were clarified by centrifugation (23500g, 60 min), and the supernatant was passed through a 0.22  $\mu\text{m}$  spin filter. A 0.2 mL sample was analyzed on a Superose 12 gel filtration column. This column was eluted with 20 mM Hepes and 300 mM NaCl (pH 7.3) buffer at a flow rate of 0.4 mL/min. Fractions were collected every minute and counted on a  $\gamma$  counter. The low molecular weight fractions for the CPTA conjugate were further analyzed by radio-TLC.

## RESULTS

The specific activities of the 1A3 conjugates were 2.3–2.6  $\mu\text{Ci}/\mu\text{g}$ , while the specific activities of the 1A3-F(ab')<sub>2</sub> conjugates ranged between 1.6 and 3.2  $\mu\text{Ci}/\mu\text{g}$ . The specific activities were not optimized to achieve their maximums. All radiolabeled conjugates were purified using either spin column purification or centricon 30 molecular weight membrane filters and shown to be >95% pure by gel filtration chromatography.

The immunoreactivity (IR) values for the  $^{64,67}\text{Cu}$ -chelate-1A3 and  $^{64,67}\text{Cu}$ -chelate-1A3-F(ab')<sub>2</sub> conjugates ranged between 75% and 90%, with the SCN-TETA conjugates having the lowest IRs of 75% and the PCBA-1A3-F(ab')<sub>2</sub> conjugate having the highest IRs of 90%. The number of chelates conjugated to the mAbs (or the chelate:mAb ratio) for all conjugates were determined using isotopic dilution methods (17). Specific activities, immunoreactivities, and chelate:mAb ratios are summarized in Table 1. The stability of the copper labeled ligands when challenged with a 10-fold excess of non-radioactive copper is summarized in Table 2. Both  $^{67}\text{Cu}$ -CPTA and  $^{67}\text{Cu}$ -PCBA showed no loss of copper for at least 48 h;  $^{67}\text{Cu}$ -TETA shows a rapid initial loss of copper at 2 h and then a slower rate of copper loss over the next 5 days.  $^{67}\text{Cu}$ -TETA was used to represent the

**Table 1. Specific Activity, Immunoreactivity, and Chelate to Antibody Ratios of the Various Conjugates Labeled with  $^{64,67}\text{Cu}$  ( $N \geq 3$ )**

conjugates	specific activity (mCi/mg)	immuno-reactivity (%)	chelate/MAB
BAT-1A3	2.5 $\pm$ 1.1	84.4 $\pm$ 4.1	1.8 $\pm$ 0.2
BAT-1A3-F(ab') <sub>2</sub>	2.7 $\pm$ 0.3	83.3 $\pm$ 3.8	1.4 $\pm$ 0.2
SCN-1A3	2.6 $\pm$ 0.04	75.4 $\pm$ 13.2	0.24 $\pm$ 0.02
SCN-1A3-F(ab') <sub>2</sub>	3.2 $\pm$ 0.8	75.3 $\pm$ 14.1	0.14 $\pm$ 0.02
CPTA-1A3	2.3 $\pm$ 0.9	84.1 $\pm$ 12.7	1.4 $\pm$ 0.2
CPTA-1A3-F(ab') <sub>2</sub>	2.3 $\pm$ 1.1	80.6 $\pm$ 5.1	2.9 $\pm$ 0.5
PCBA-1A3	2.6 $\pm$ 0.1	84.1 $\pm$ 3.7	1.4 $\pm$ 0.2
PCBA-1A3-F(ab') <sub>2</sub>	1.6 $\pm$ 0.7	90.0 $\pm$ 4.2	0.7 $\pm$ 0.1

**Table 2. Structural and Thermodynamic Parameters, Lipophilicity, and Charge of the Bifunctional Chelates Evaluated in This Study<sup>a</sup>**

bifunctional chelate	BAT	SCN-TETA	CPTA	PCBA
type of bond formed	thioether	thiourea	amide	amide
complex charge	2–	2–	1+	1+
Hansch lipophilicity relative to CPTA = 5.00	1.46	1.32	5.00	2.85
$\Delta \log K$ (Cu-Zn)	5.3	5.3	11.7	9.2
$\Delta \log K$ (Cu-Ca)	13.3	13.3		
$\Delta \log K$ (Cu-Mg)	19.6	19.6		
% of $^{64,67}\text{Cu}$ displaced by Cu(II) after 2 days	70	70	15	5

<sup>a</sup> The  $\Delta \log K$  values are presented for the metal–macrocyclic complexes and not the metal–BFC complexes.

stability of  $^{67}\text{Cu}$ -BAT and  $^{67}\text{Cu}$ -SCN-TETA toward non-radioactive Cu(II) displacement because the  $\alpha$ -keto-bromo group of BAT and the isothiocyanato group from SCN-TETA were found to be too reactive for reliable chromatography.

**Animal Biodistribution Studies.** The  $^{64}\text{Cu}$ -labeled mAb conjugates were evaluated and compared in normal rats and in the tumor-bearing hamsters. Rat and hamster biodistributions of the Cu-labeled 1A3 conjugates at 24 h post-injection are shown in Figure 2. Liver and kidney uptake in rats was significantly lower for  $^{64}\text{Cu}$ -BAT-2IT-1A3 than for the other conjugates ( $p$  values of <0.02 and <0.03, respectively). Tumor uptake in hamsters was high at 24 h for all conjugates except for  $^{64}\text{Cu}$ -CPTA-1A3 ( $p$  values of <0.04). In the hamsters, the liver and kidney uptake was similar for all of the conjugates.

Rat and hamster biodistributions of 1A3-F(ab')<sub>2</sub> conjugated with the four bifunctional chelates at 24 h post-injection are shown in Figure 3. Liver uptake in rats (%ID/g) was lowest for  $^{64}\text{Cu}$ -BAT-2IT-1A3-F(ab')<sub>2</sub> and  $^{64}\text{Cu}$ -SCN-TETA-1A3-F(ab')<sub>2</sub>, and both were significantly different from  $^{64}\text{Cu}$ -CPTA-1A3-F(ab')<sub>2</sub> and  $^{64}\text{Cu}$ -PCBA-1A3-F(ab')<sub>2</sub> ( $p$  values of <0.02). Kidney uptake in rats (%ID/g) was also lowest for  $^{64}\text{Cu}$ -BAT-2IT-1A3-F(ab')<sub>2</sub> (13.57  $\pm$  2.56) and  $^{64}\text{Cu}$ -SCN-TETA-1A3-F(ab')<sub>2</sub> (15.35  $\pm$  2.55), and both were lower than  $^{64}\text{Cu}$ -CPTA-1A3-F(ab')<sub>2</sub> (27.58  $\pm$  2.25) and  $^{64}\text{Cu}$ -PCBA-1A3-F(ab')<sub>2</sub> (23.83  $\pm$  1.89) ( $p$  values of <0.002). Hamsters showed a similar pattern with liver uptake being significantly lower for  $^{64}\text{Cu}$ -BAT-2IT-1A3-F(ab')<sub>2</sub> (1.68  $\pm$  0.31) and  $^{64}\text{Cu}$ -SCN-TETA-1A3-F(ab')<sub>2</sub> (1.27  $\pm$  0.10) than  $^{64}\text{Cu}$ -CPTA-1A3-F(ab')<sub>2</sub> (2.71  $\pm$  0.47) and  $^{64}\text{Cu}$ -PCBA-1A3-F(ab')<sub>2</sub> (3.00  $\pm$  0.67) ( $p$

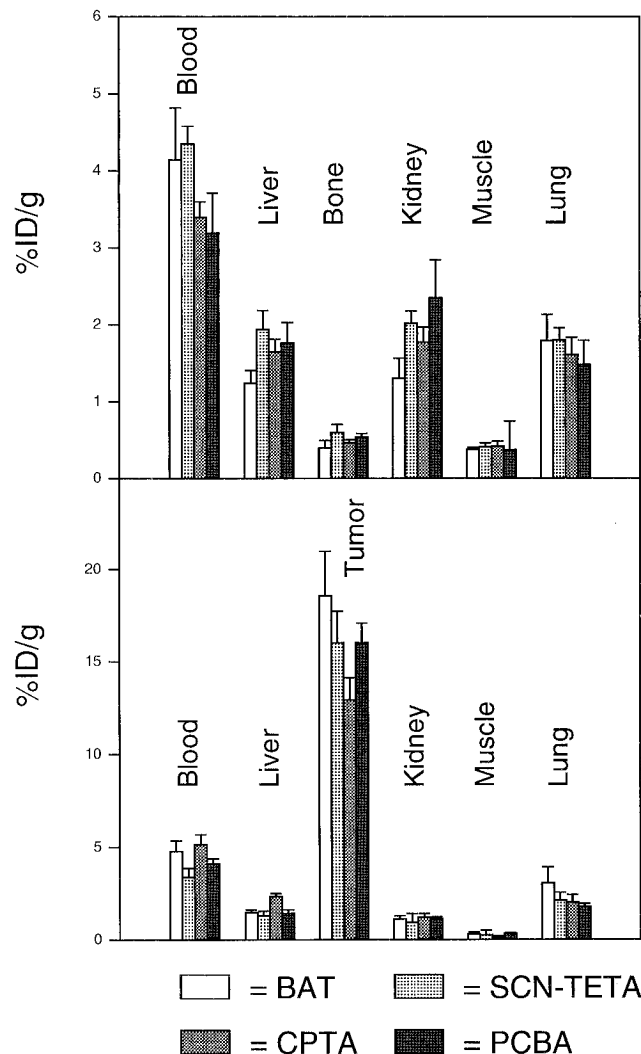


**Figure 2.** Biodistribution data for  $^{64}\text{Cu}$ -BFC-1A3 conjugates in Sprague-Dawley rats (top) and tumor-bearing Golden Syrian hamsters (bottom) at 24 h post-injection. Data are presented as the mean plus or minus the standard deviation of  $n \geq 4$ .

values of  $<0.002$ ). In hamsters, kidney uptake of  $^{64}\text{Cu}$ -BAT-2IT-1A3-F(ab')<sub>2</sub> ( $7.99 \pm 0.84$ ) and  $^{64}\text{Cu}$ -SCN-TETA-1A3-F(ab')<sub>2</sub> ( $3.35 \pm 0.60$ ) was also lower than  $^{64}\text{Cu}$ -CPTA-1A3-F(ab')<sub>2</sub> ( $23.57 \pm 2.41$ ) and  $^{64}\text{Cu}$ -PCBA-1A3-F(ab')<sub>2</sub> ( $17.56 \pm 2.71$ ) ( $p$  values of  $<4 \times 10^{-6}$ ). Furthermore, in hamster liver and kidneys,  $^{64}\text{Cu}$ -SCN-TETA-1A3-F(ab')<sub>2</sub> was significantly lower than  $^{64}\text{Cu}$ -BAT-2IT-1A3-F(ab')<sub>2</sub> ( $p$  values of  $<0.04$  and  $<7 \times 10^{-6}$ , respectively). Tumor uptake for all of the conjugates was high (between 8.2% and 13.7% ID/g).

Blood clearance data for the  $^{64}\text{Cu}$ -labeled 1A3 and 1A3-F(ab')<sub>2</sub> conjugates are shown in Figure 4. The Cu-labeled 1A3-F(ab')<sub>2</sub> conjugates cleared more rapidly than the Cu-labeled 1A3 conjugates. All of the intact conjugates had similar blood clearance patterns; however,  $^{64}\text{Cu}$ -PCBA-1A3 had the lowest concentration in the blood at all time points. There were greater differences in blood clearance among the 1A3-F(ab')<sub>2</sub> conjugates;  $^{64}\text{Cu}$ -CPTA-1A3-F(ab')<sub>2</sub> and  $^{64}\text{Cu}$ -PCBA-1A3-F(ab')<sub>2</sub> cleared more rapidly from the blood than  $^{64}\text{Cu}$ -BAT-2IT-1A3-F(ab')<sub>2</sub> and  $^{64}\text{Cu}$ -SCN-TETA-1A3-F(ab')<sub>2</sub>.

**Gel Filtration Chromatography of Liver and Kidney Metabolites.** The liver metabolism data for  $^{67}\text{Cu}$ -labeled BFC-1A3 conjugates are summarized in Table 3. Liver metabolites from the control rats (injected with  $^{67}\text{Cu}$  acetate) showed  $>90\%$  of the radioactivity eluted in a peak corresponding to a MW of  $\sim 35$  kDa at

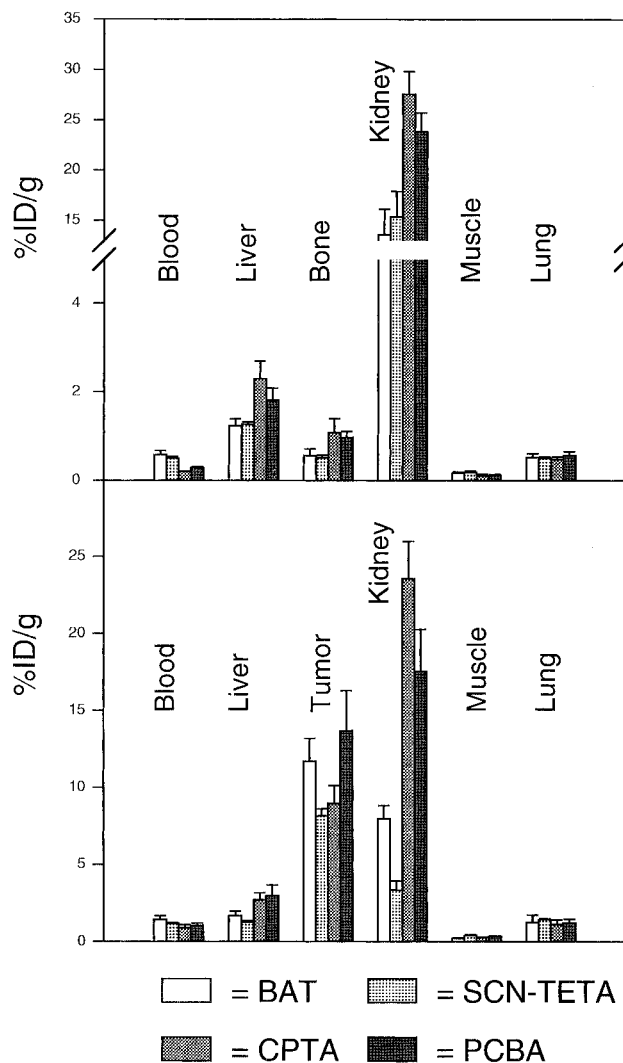


**Figure 3.** Biodistribution data for  $^{64}\text{Cu}$ -BFC-1A3-F(ab')<sub>2</sub> conjugates in Sprague-Dawley rats (top) and tumor-bearing Golden Syrian hamsters (bottom) at 24 h post-injection. Data are presented as the mean plus or minus the standard deviation of  $n \geq 3$ .

1, 3, and 5 day time points (Figure 5). Analysis of liver homogenates from rats injected with  $^{67}\text{Cu}$ -labeled 1A3 conjugates at 1 day post-injection showed that the majority of the  $^{67}\text{Cu}$  was associated with intact mAb. For example, at 1 day post-injection, 74% of the radioactivity from rats injected with  $^{67}\text{Cu}$ -CPTA-1A3 remained associated with the intact antibody peak (Figure 6). There was also a component that eluted with a MW of 35 kDa (12%) and a low molecular weight component ( $<5$  kDa) (14%). At the later time points, the amount of radioactivity associated with intact antibody decreased (48% at 5 days), while the other two metabolites increased (28% and 24%, respectively). The  $^{67}\text{Cu}$ -PCBA-1A3 liver homogenate gel filtration profile at day 1 was similar to  $^{67}\text{Cu}$ -CPTA-1A3 at day 1, with 73% of the activity being antibody associated and the rest of the activity being primarily associated with a component having a MW of 35 kDa (26%). At days 3 and 5, the  $^{67}\text{Cu}$ -PCBA-1A3 liver metabolite of 35 kDa increased to 59% and 70%, respectively, while the intact mAb peak decreased to 24% by day 5. In the rat liver, the  $^{67}\text{Cu}$ -SCN-TETA-1A3 conjugate was  $>90\%$  intact at 1 day with the remaining activity eluting with a MW of 35 kDa (8%). By day 5, 43% of the total activity was mAb associated and the remaining metabolites eluted with MWs of 35 kDa (41%) and  $<5$  kDa (16%).

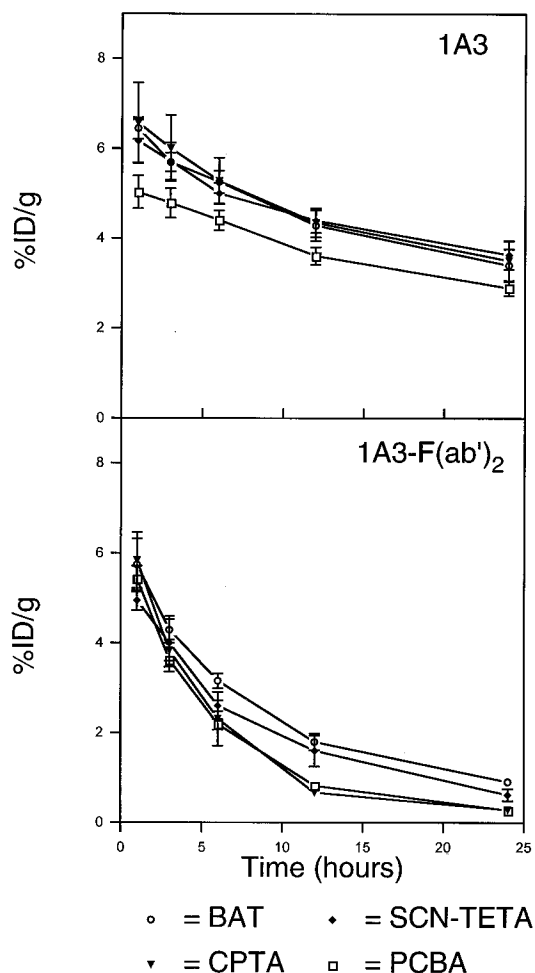


**Figure 4.** Blood clearance in Sprague-Dawley rats of the various  $^{64}\text{Cu}$ -labeled 1A3 conjugates (top) and  $^{64}\text{Cu}$ -labeled 1A3-F(ab) $_2$  conjugates (bottom). Data are presented as the mean plus or minus the standard deviation of  $n \geq 3$ .

The renal metabolites of Sprague-Dawley rats injected with  $^{67}\text{Cu}$ -CPTA-1A3-F(ab) $_2$ ,  $^{67}\text{Cu}$ -PCBA-1A3-F(ab) $_2$ ,  $^{67}\text{Cu}$ -SCN-TETA-1A3-F(ab) $_2$ , and  $^{67}\text{Cu}$  acetate as a control were analyzed at 1, 3, and 5 days. The rats injected with  $^{67}\text{Cu}$  acetate showed two major peaks at day 1, one eluting with a MW of 35 kDa (40%) and one eluting with a MW of 10 kDa (40%). By days 3 and 5, most of the activity was associated with the 35 kDa peak (85% and 90%, respectively), while the rest of the activity eluted with the low molecular weight (<5 kDa) peak (15% and 10%, respectively).  $^{67}\text{Cu}$ -CPTA-1A3-F(ab) $_2$  was completely metabolized to a low molecular weight species (<5 kDa) by 1 day post-injection (Figure 6). Both  $^{67}\text{Cu}$ -PCBA-1A3-F(ab) $_2$  and  $^{67}\text{Cu}$ -SCN-TETA-1A3-F(ab) $_2$  were also >85% converted to a low (<5 kDa) molecular weight species by 1 day post-injection. A peak (<5%) with a MW of 35 kDa appeared at day 5 for both of these conjugates.

**Gel Filtration Chromatography of  $^{64}\text{Cu}$ -SOD.** The gel filtration chromatogram of  $^{64}\text{Cu}$ -SOD showed that all of the activity eluted with a MW of 35 kDa (Figure 5). This coincides with the peak from the liver metabolism of rats injected with CuOAc.

**Thin Layer Chromatography of Metabolites.** The low molecular weight metabolites for the CPTA conjugate at day 1 were collected from the size exclusion chromatography experiment and further analyzed by radio-TLC. Samples were either mixed with  $^{67}\text{Cu}$ -CPTA- $\epsilon$ -lysine or  $^{67}\text{Cu}$ -CPTA standards and applied to glass backed silica gel plates. Both liver and kidney metabolites co-migrated

with the  $^{67}\text{Cu}$ -CPTA- $\epsilon$ -lysine standard (Figure 7). These metabolites migrated separately from the  $^{67}\text{Cu}$ -CPTA standard.

## DISCUSSION

CPTA and PCBA were synthesized as previously described (21, 35). The synthesis of BAT was first described by Moi et al. (32); however, an improved synthesis of BAT has been described by Moran et al. that gives the final product in 23% yield (33). A combination of these procedures, along with some minor modifications (38), yielded BAT and SCN-TETA in comparable yields. CPTA- $\epsilon$ -lysine is a new compound that was synthesized as a standard for the metabolism studies by an adaptation of the solid-phase method of Franano et al. (29) without the optimization of yield.

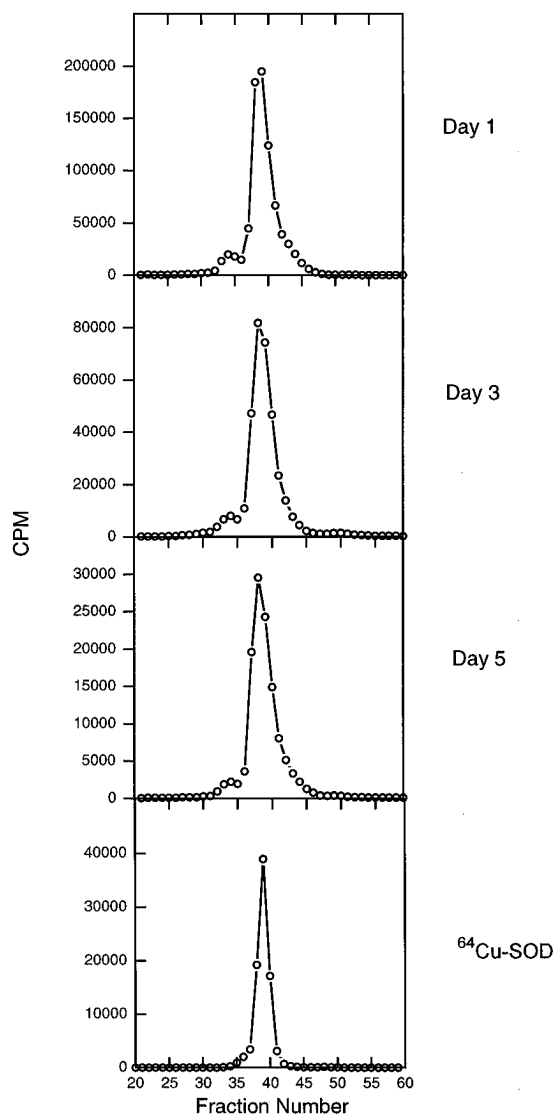
The conjugation and purification of the BAT-2IT-1A3 conjugate was straightforward; however, the presence of 2IT with 1A3-F(ab) $_2$  fragments reduced disulfide bonds, producing a smaller fragment with a molecular weight of 55 kDa and low IR (17). Therefore, FPLC purification of the BAT-2IT-1A3-F(ab) $_2$  conjugates was necessary prior to labeling to remove the 55 kDa fragments (17). The conjugation and purification of SCN-TETA to both 1A3 and 1A3-F(ab) $_2$  was uncomplicated, and size exclusion chromatography showed no breakdown of the intact mAb or fragments; however, the IR of the SCN-TETA conjugates was significantly lower than those of the other conjugates, and only after optimization of the SCN-TETA:mAb ratio and pH were the  $^{67}\text{Cu}$ -SCN-TETA conjugates acceptable for *in vivo* studies. The conjugation of CPTA and PCBA to mAbs was straightforward, and the Cu-labeled conjugates had IRs > 80%.

There were differences in biodistribution trends between rats and hamsters. In Sprague-Dawley rats,  $^{64}\text{Cu}$ -BAT-2IT-1A3 had the lowest uptake in both the liver and kidneys at 24 h. In hamsters, significantly lower uptake in the kidneys of  $^{64}\text{Cu}$ -SCN-TETA 1A3-F(ab) $_2$  compared to the other conjugates was observed, and this result was not observed in rats. The differences between the two rodent species are not totally understood. A possible explanation may be the different copper binding protein levels in rats and hamsters. The concentrations of these copper binding proteins may affect their biodistribution by transchelation of the copper. Owen showed that different copper binding proteins are present in different concentrations for the same organ in different animal species (41). In most animal species, there are three major copper binding proteins (42): metallothionein (6 kDa), superoxide dismutase (32 kDa), and ceruloplasmin (124 kDa). Protein concentrations also differ between tissues in the same species. Van Hein et al. showed that there is twice as much superoxide dismutase in the liver of a rat than in any other tissue (43).

The differences between  $^{64}\text{Cu}$ -BAT-2IT-1A3 and  $^{64}\text{Cu}$ -SCN-TETA-1A3 in the liver and kidneys imply that the different linking moieties (thioether vs thiourea) affected the accumulation/retention of activity at these sites. These two bifunctional chelates have the same copper macrocycle, hence the same log *K* and charge, and similar lipophilicities. Therefore, the major difference may be the rate of cleavage of the thiourea bond versus the thioether (44-46). The biodistribution differences between the four  $^{64}\text{Cu}$ -BFC-1A3-F(ab) $_2$  conjugates were notable in both rats and hamsters (Figure 3). The uptake of  $^{64}\text{Cu}$ -BAT-2IT-1A3-F(ab) $_2$  and  $^{64}\text{Cu}$ -SCN-TETA-1A3-F(ab) $_2$  were significantly lower in the liver and kidneys of both rats and hamsters than the uptake of  $^{64}\text{Cu}$ -CPTA-1A3-F(ab) $_2$  and  $^{64}\text{Cu}$ -PCBA-1A3-F(ab) $_2$ . This could be

**Table 3. Summary of Size Exclusion Chromatography Data for  $^{67}\text{Cu}$ -BFC-1A3 Liver Metabolites: Percent of Radioactivity Associated with Three Major Components**

	intact antibody (150 kDa)			35 kDa			<5 kDa		
	day 1	day 3	day 5	day 1	day 3	day 5	day 1	day 3	day 5
SCN-TETA	91	48	43	8	40	41	1	12	16
CPTA	74	58	48	12	22	28	14	20	24
PCBA	73	32	24	26	59	70	1	9	6

**Figure 5.** Size exclusion FPLC profiles of  $^{67}\text{Cu}$ OAc liver metabolites at 1, 3, and 5 days post-injection and of  $^{64}\text{Cu}$ -SOD. Counts per minute (cpm) are plotted versus the fraction number. Note: Fractions 1–20 are the void volume.

due to the lipophilicity and/or charge differences between the BAT/SCN-TETA and the CPTA/PCBA chelates. If the mAbs are metabolized to the Cu(II)-BFC or Cu(II)-BFC-amino acid moieties, the more lipophilic and/or positively charged metabolites are likely to accumulate in the liver and kidneys and not clear as rapidly (47, 48).

Lipophilicities of the copper chelates, as determined by octanol/water partition coefficient ( $\log P$ ) measurements, were not evaluated experimentally due to the low extraction of these complexes into octanol. Since the actual  $\log P$  values are likely negative values, due to the charge on the complexes, only relative lipophilicities could be determined by the Hansch method (49). Cu(II)-CPTA was the most lipophilic complex and was assigned an arbitrary  $\log P$  value of 5.00. According to Hansch, Cu(II)-BAT and Cu(II)-SCN-TETA are the least lipophilic and Cu(II)-PCBA is intermediate between these com-

plexes and Cu(II)-CPTA (Table 2). At physiologic pH, Cu(II) complexes of BAT and SCN-TETA have a charge of negative two ( $2^-$ ), while Cu(II) complexes of CPTA and PCBA have a charge of positive one ( $1^+$ ) (21). The facts that positively charged compounds are known to accumulate in the kidneys (50) and that Cu(II) complexes of CPTA and PCBA are relatively lipophilic may account for their high kidney uptake. Also, differences in the stability of the copper complexes between TETA and CPTA/PCBA may provide an alternate or additional explanation.

The biodistribution differences within a species may be partially due to differences in stability of the Cu-BFC complex. The least stable Cu(II)-BFC complexes are more readily dissociated *in vivo*. One possible mechanism for the release of copper from the bifunctional chelate would be the replacement of copper by other metals present in the body. The difference in stability ( $\Delta \log K$ ) between the Cu(II) complex with that of other metal ions would be a measure of the ease of transchelation. The  $\Delta \log K$  values for the various chelates macrocyclic portion (TETA, cyclam, 15aneN5) in Table 2 were derived from literature values (51). All of the Cu(II)-chelate complexes are more stable than the complexes formed with the other biologically related metals. This agrees with an *in vitro* study by Kukis et al. that showed that an antibody-TETA conjugate had a higher selectivity for Cu(II) than for Zn(II), Ca(II), or Mg(II) (52). The Cu-labeled BAT and SCN-TETA conjugates are retained less in the liver and kidneys than those of CPTA and PCBA, yet the  $\Delta \log K$  for Cu-Zn is larger for CPTA and PCBA than for BAT and SCN-TETA. These data suggest that displacement of Cu(II) by another metal ion is unlikely. Another explanation is that the  $^{64,67}\text{Cu}$  can be displaced by non-radioactive copper. Our data from experiments where the Cu-labeled BFCs were challenged with non-radioactive Cu(II) showed that  $\sim 70\%$  of the  $^{64,67}\text{Cu}$  in the TETA complex was displaced by cold Cu(II) at 2 days, whereas  $< 15\%$  of  $^{64,67}\text{Cu}$ -CPTA and PCBA were displaced by cold Cu(II) at 2 days. If  $^{64,67}\text{Cu}$  was released from the BAT or SCN-TETA conjugates in the liver and kidneys, it would be likely that the  $^{64,67}\text{Cu}$  would quickly bind to copper binding proteins and remain trapped in those organs rather than be cleared. Since the  $^{64,67}\text{Cu}$ -TETA conjugates have the most rapid clearance from liver and kidneys, it is unlikely that  $^{64,67}\text{Cu}$  is being displaced by cold Cu(II) *in vivo*.

The metabolism *in vivo* of  $^{111}\text{In}$ -labeled polypeptides and mAbs has been investigated (12, 24, 26–30). Previous studies have shown that  $^{111}\text{In}$ -labeled mAbs are degraded to small molecular weight metabolites (24, 26, 30). These studies have indicated that the major small molecular weight metabolite formed was  $^{111}\text{In}$ -BFC- $\epsilon$ -lysine, a result of proteolysis of the amino acid backbone of the protein. Thus, it is likely that the major metabolite of the Cu-labeled mAbs is  $^{64,67}\text{Cu}$ -BFC- $\epsilon$ -lysine. By investigating the nature of the metabolite of the different Cu-labeled BFC-mAb conjugates, the cause for the resulting differences in the biodistribution may be elucidated.

The size exclusion data of all  $^{67}\text{Cu}$ -BFC-1A3-F(ab) $_2$  kidney metabolites show that, by 1 day post-injection,

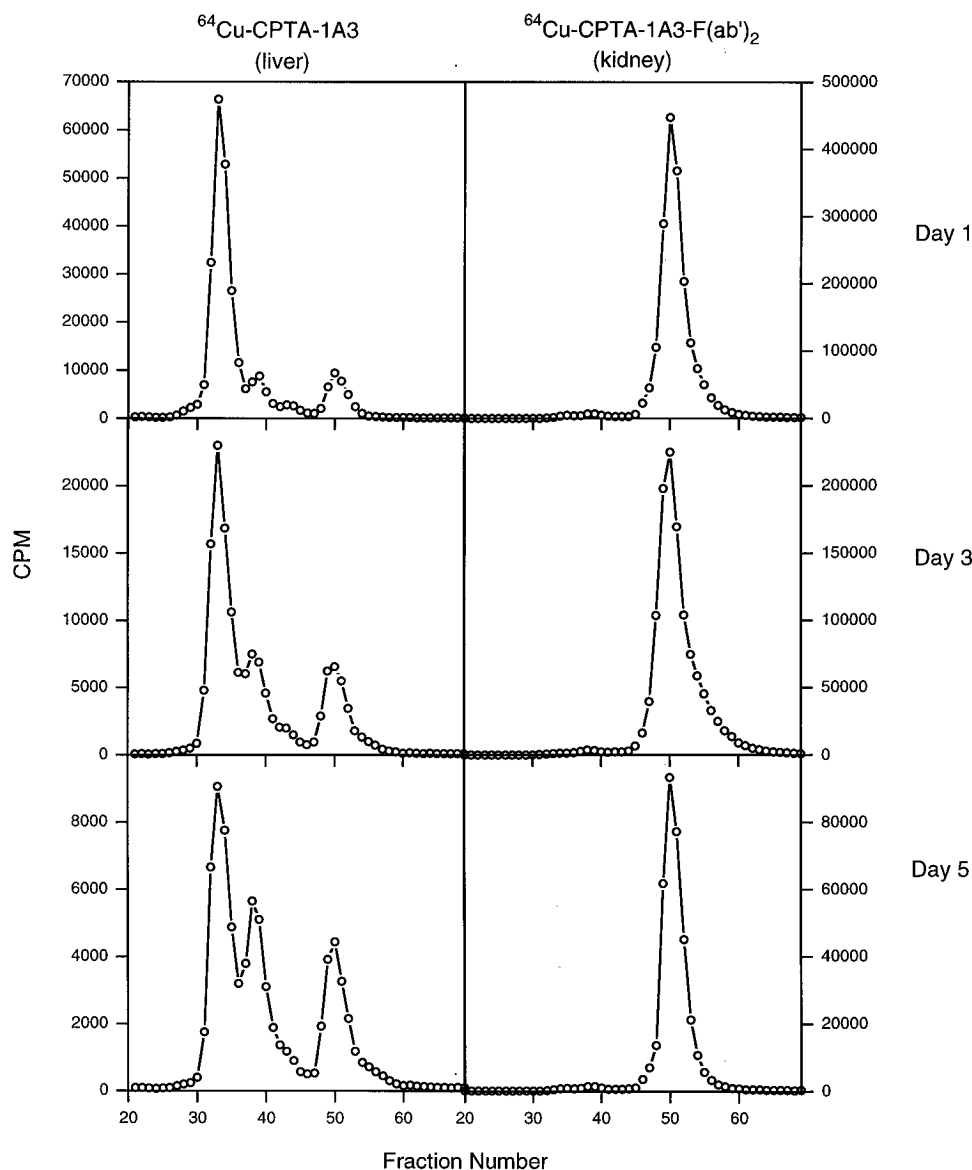


**Figure 6.** Size exclusion FPLC profiles of  $^{67}\text{Cu}$ -CPTA-1A3 liver metabolites (left) and  $^{67}\text{Cu}$ -CPTA-1A3-F(ab')<sub>2</sub> kidney metabolites (right) at 1, 3, and 5 days post-injection. Counts per minute (cpm) are plotted versus the fraction number. Note: Fractions 1–20 are the void volume.

>85% of the activity was associated with the low (<5 kDa) molecular weight species. This agrees with the  $^{111}\text{In}$ -mAb data (30) and suggests that the  $^{64/67}\text{Cu}$ -labeled BFC-1A3-F(ab')<sub>2</sub> conjugates are efficiently deposited within lysosomes by absorptive endocytosis and that subsequent lysosomal degradation was rapid (53). These data suggest that smaller radiolabeled mAbs and peptides may have the same kidney uptake and lysosomal retention as a F(ab')<sub>2</sub> fragment due to the high kidney activity seen with these smaller compounds (54–56). Also, metabolizable linkers may not be a solution to the problem of high renal accumulation unless the radiolabel is prevented from reaching the lysosome or the radiolabeled metabolite is in a form in which it can be rapidly exported from the lysosome.

The  $^{67}\text{Cu}$ -PCBA-1A3-F(ab')<sub>2</sub> and  $^{67}\text{Cu}$ -SCN-TETA-1A3-F(ab')<sub>2</sub> kidney metabolism data demonstrated the appearance of a minor peak (<10%) with a molecular weight of ~35 kDa at 5 days. This corresponded to the same molecular weight peak observed for the rats injected with  $^{67}\text{Cu}$  acetate. This suggests that, after several days, Cu(II) was dissociated from the conjugates and then bound to a 35 kDa protein *in vivo*.

The results of the  $^{67}\text{Cu}$ -labeled 1A3 liver homogenates were more complicated than those of the  $^{67}\text{Cu}$ -labeled 1A3-F(ab')<sub>2</sub> kidney homogenates. All of the intact 1A3 conjugates showed a similar pattern; at 1 day post-injection, the majority of radioactivity was associated with the intact antibody peak (MW = 150 kDa). At later time points, an increasing amount of activity eluted with a molecular weight of ~35 kDa. In addition, the  $^{67}\text{Cu}$ -BFC-1A3 liver homogenates showed a low molecular weight peak that increased over the 5 day period. These results differ from the  $^{111}\text{In}$ -labeled glycoprotein data (28) and the  $^{111}\text{In}$ - and  $^{67}\text{Cu}$ -labeled 1A3-F(ab')<sub>2</sub> data, which showed a rapid conversion to a low molecular weight species; however, the results agree with  $^{111}\text{In}$ -labeled 1A3 metabolism data (30). The fact that  $^{67}\text{Cu}$ -labeled 1A3 conjugates did not rapidly metabolize to a low molecular weight species (<5 kDa) in the liver suggests that they were not targeted to cell surface receptors and lack an effective uptake mechanism, such as absorptive endocytosis in the kidneys.

At 1 day post-injection, only  $^{67}\text{Cu}$ -CPTA-1A3 was partially metabolized in the liver to a low molecular weight species. TLC of the low molecular weight species

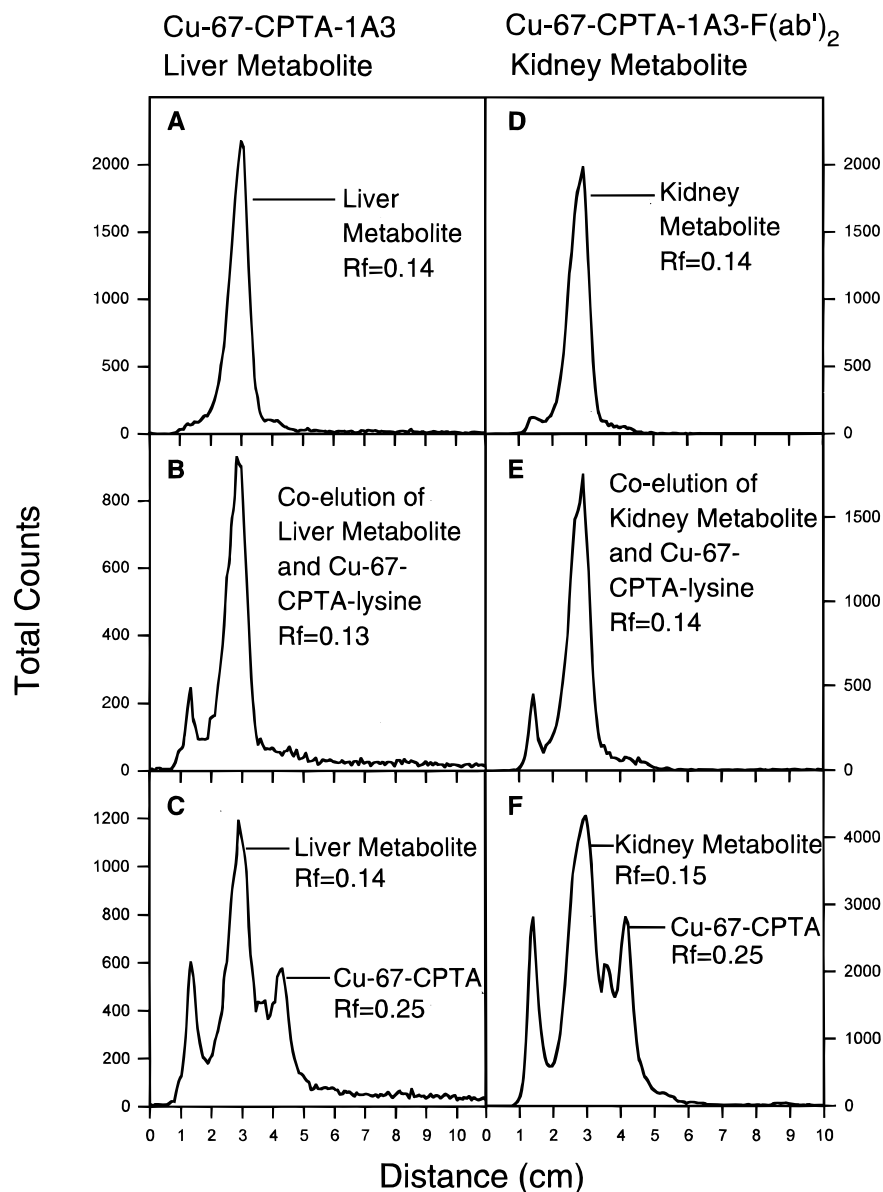


**Figure 7.** Silica gel radio-TLC of the small molecular weight metabolites for  $^{67}\text{Cu}$ -CPTA-1A3 and  $^{67}\text{Cu}$ -CPTA-1A3-F(ab')<sub>2</sub> (1 day post-injection) collected by size exclusion chromatography.  $^{67}\text{Cu}$ -CPTA-1A3 metabolites are shown alone (A), mixed with  $^{67}\text{Cu}$ -CPTA- $\epsilon$ -lysine standard (B), and with  $^{67}\text{Cu}$ -CPTA standard (C).  $^{67}\text{Cu}$ -CPTA-1A3-F(ab')<sub>2</sub> metabolites are shown alone (D), with  $^{67}\text{Cu}$ -CPTA- $\epsilon$ -lysine standard (E), and with  $^{67}\text{Cu}$ -CPTA standard (F). The origin for all plates is 1 cm.

from  $^{67}\text{Cu}$ -CPTA-1A3 liver metabolites and  $^{67}\text{Cu}$ -CPTA-1A3-F(ab')<sub>2</sub> kidney metabolites identified the species as  $^{67}\text{Cu}$ -CPTA- $\epsilon$ -lysine (Figure 7). The appearance of the low molecular weight peak for the  $^{67}\text{Cu}$ -CPTA-1A3 conjugate, along with the previous data on antibody metabolism (57–60), suggest that the  $^{67}\text{Cu}$ -CPTA-1A3 conjugate was partially degraded in the lysosome. The mAb could also localize in extracellular sites and bind non-specifically to surface molecules or be internalized by specific (Fc receptor) or nonspecific (fluid-phase endocytosis) means.

The size exclusion data for  $^{67}\text{Cu}$ -PCBA-1A3 and  $^{67}\text{Cu}$ -SCN-TETA-1A3 did not show a low molecular weight peak (<1%) at day 1. This might suggest that the radiolabel was not delivered to the lysosome for degradation; however, it is more likely that the  $^{67}\text{Cu}$  transchelated to a protein with a larger molecular weight prior to localization in the lysosome.

In the liver, all of the Cu-labeled 1A3 conjugates were partially metabolized to a 35 kDa species. There are two possible explanations for this: first, the radiolabeled antibody may have been partially degraded within en-

dosomes (58–61), giving the intermediate molecular weight peak of 35 kDa; however, this is not in agreement with  $^{111}\text{In}$ -labeled mAb studies which show a broadening of the intact mAb peak and the absence of a peak at 35 kDa (30). Alternatively, Cu(II) could be released from the chelate and bind to a 35 kDa protein. The size exclusion data of liver homogenates from rats injected with  $^{67}\text{Cu}$  acetate showed that the  $^{67}\text{Cu}$  activity elutes at a molecular weight of 35 kDa, which gives credence to the latter argument. The liver contains a 32 kDa enzyme, superoxide dismutase (SOD), which has one Cu(II) ion per active site (42). The concentration of SOD in the rat liver is twice as great as in any other tissue (43). SOD has been labeled with  $^{64}\text{Cu}$  and analyzed by size exclusion chromatography and was found to co-migrate with the 35 kDa peak observed in the liver metabolism of  $^{67}\text{Cu}$  acetate and  $^{67}\text{Cu}$ -BFCs-1A3. Thus, it appears that transchelation of Cu(II) from the 1A3 conjugates to SOD is a reasonable explanation for the 35 kDa peak. Definitive confirmation of the identity of the 35 kDa metabolite is underway.

The rate at which the radiolabeled intact antibody peak

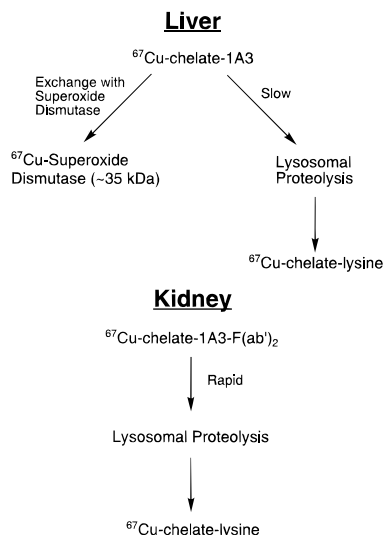


**Figure 8.** Proposed mechanisms for the uptake and retention of  $^{64/67}\text{Cu}$ -labeled 1A3 in the liver (A) and  $^{64/67}\text{Cu}$ -labeled 1A3-F(ab')<sub>2</sub> in the kidneys (B).

was converted to the 35 kDa species in the rat liver also differed between the conjugates. For  $^{67}\text{Cu}$ -CPTA-1A3 and  $^{67}\text{Cu}$ -SCN-TETA-1A3 at day 5, 28% and 41% of the activity was associated with the 35 kDa peak, respectively, while 70% of the activity for  $^{67}\text{Cu}$ -PCBA-1A3 was associated with this peak. This suggests that the rate of transchelation of  $^{67}\text{Cu}$  from PCBA-1A3 to a 35 kDa protein was more rapid than that of the  $^{67}\text{Cu}$ -CPTA-1A3 and  $^{67}\text{Cu}$ -SCN-TETA-1A3 conjugates. These data do not correlate with the stability of the complexes, which shows Cu-PCBA as stable a complex as Cu-CPTA and more stable than Cu-TETA (21). We are currently carrying out experiments to elucidate the liver metabolism of other  $^{64/67}\text{Cu}$ -BFC-proteins in order to better interpret these results.

It is more difficult to correlate the biodistribution of the Cu-labeled BFC-1A3 conjugates with the metabolite data, since the differences in liver uptake between the four intact mAb conjugates are not as significant as those of the Cu-labeled BFC-1A3-F(ab')<sub>2</sub> uptake in the kidney. Retention of Cu-labeled BFC-1A3 conjugates in the liver is probably a result of transchelation of radioactive Cu(II) to copper binding proteins, such as SOD in the liver (Figure 8). In the kidney,  $^{64}\text{Cu}$ -CPTA-1A3-F(ab')<sub>2</sub> and  $^{64}\text{Cu}$ -PCBA-1A3-F(ab')<sub>2</sub> had nearly a 2-fold higher uptake over that of  $^{64}\text{Cu}$ -SCN-TETA-1A3-F(ab')<sub>2</sub> in rats, and an even greater increased uptake in tumor-bearing hamsters. The kidney metabolism of the  $^{67}\text{Cu}$ -BFC-1A3-F(ab')<sub>2</sub> conjugates showed a rapid conversion to small molecular weight metabolites (< 5 kDa) by 1 day post-injection. This suggests that proteolysis of mAb fragments resulted in the small molecular weight lysine or N-terminal amino acid derivatives of the bifunctional chelates (Figure 8). The observed biodistribution differences are most likely due to the resulting charge and/or lipophilicity of these derivatives, which dictate the uptake and clearance from the organ (48).

In summary, the purpose of this study was to correlate biodistribution of  $^{64/67}\text{Cu}$ -labeled intact MAb and MAb F(ab')<sub>2</sub> fragments in a rat model to metabolism in nontarget organs such as the liver and kidneys. The liver metabolism of  $^{67}\text{Cu}$ -labeled BFC-1A3 conjugates was slow, and it appears that  $^{67}\text{Cu}$  was transchelated to a 35 kDa protein (possibly SOD). The metabolism of  $^{67}\text{Cu}$ -labeled BFC-1A3-F(ab')<sub>2</sub> conjugates was rapid in the kidneys, and chromatographic results for  $^{67}\text{Cu}$ -CPTA-1A3-F(ab')<sub>2</sub> suggest that  $^{67}\text{Cu}$ -BFC- $\epsilon$ -lysine was the major

metabolite. Therefore, chelate charge and lipophilicity of a  $^{64/67}\text{Cu}$ -BFC-amino acid metabolite play a large role in kidney retention, while transchelation of the copper label to a protein appears to be a major factor for liver accumulation.

The understanding of the mechanisms for accumulation of radiometal-labeled BFC-mAb conjugates in nontarget organs is vital for the design of effective imaging and radioimmunotherapy agents. The research presented here is a first step in determining the metabolism of mAbs labeled with copper radioisotopes. The mechanisms of radiolabel accumulation in the liver and kidney that are presented here help to explain the observed biodistribution results; however, more work needs to be done to verify these mechanisms.

#### ACKNOWLEDGMENT

The authors would like to thank Henry Lee for his technical assistance and Dr. James R. Duncan for helpful discussions concerning the metabolism of the copper labeled antibodies. This work was funded by a DOE Grant DE-FG02-87-ER60512 (MJW) and NIH Grant CA-42925.

#### LITERATURE CITED

- (1) Keenan, A. M., Harbert, J. C., and Larson, S. M. (1985) Monoclonal Antibodies in Nuclear Medicine. *J. Nucl. Med.* 26, 531-537.
- (2) Waldmann, T. A. (1991) Monoclonal Antibodies in Diagnosis and Therapy. *Science* 252, 1657-1662.
- (3) DeNardo, S., DeNardo, G., Kukis, D., Mausner, L., Moody, D., and Meares, C. (1991) Pharmacology of Cu-67-TETA-Lym-1 Antibody in Patients with B Cell Lymphoma. *Antibody, Immunoconjugates, Radiopharm.* 4, 36.
- (4) DeNardo, G. L., DeNardo, S. J., Meares, C. F., Salako, Q., Kukis, D. L., Mausner, L. F., Lewis, J. P., O'Grady, L. F., and Srivastava, S. C. (1993) Pilot Therapy of Lymphoma with Fractionated Cu-67-BAT-Lym-1. *J. Nucl. Med.* 34, 93P.
- (5) Delaloye, A. B., Buchegger, F., Smith, A., Schubiger, P. A., Maecke, H. R., Poncioni, L., Gillet, M., Mach, J. P., and Delaloye, B. (1994) Cu-67-Anti-CEA MAb, A Potential Therapeutic Agent: Biokinetic Studies in Patients with Colon Carcinoma. *J. Nucl. Med.* 35, 101P.
- (6) Philpott, G. W., Dehdashti, F., Schwarz, S. W., Connett, J. M., Anderson, C. J., Zinn, K. R., Meares, C. F., Welch, M. J., and Siegel, B. A. (1994) Positron Emission Tomography (PET) with Cu-64-Labeled Monoclonal Antibody (MAb 1A3) in Colorectal Cancer. *J. Nucl. Med.* 35, 12P.
- (7) Philpott, G. W., Dehdashti, F., Schwarz, S. W., Connett, J. M., Anderson, C. J., Zinn, K. R., Cutler, P. D., Welch, M. J., and Siegel, B. A. (1995) RadioimmunoPET (MAB-PET) with Cu-64-Labeled Monoclonal Antibody (MAB 1A3) Fragments [F(ab')<sub>2</sub>] in Patients with Colorectal Cancers. *J. Nucl. Med.* 36, 9P.
- (8) Philpott, G. W., Schwarz, S. W., Anderson, C. J., Dehdashti, F., Connett, J. M., Zinn, K. R., Meares, C. F., Cutler, P. D., Welch, M. J., and Siegel, B. A. (1995) RadioimmunoPET: Detection of Colorectal Carcinoma with Positron-Emitting Copper-64-Labeled Monoclonal Antibody. *J. Nucl. Med.* 36, 1818-1824.
- (9) Apelgot, S., Coppey, J., Gaudemer, A., Grisvard, J., Guille, E., Sasaki, I., and Sissoeff, I. (1989) Similar Lethal Effect in Mammalian Cells for Two Radioisotopes of Copper with Different Decay Schemes, Cu-64 and Cu-67. *Int. J. Radiat. Biol.* 55, 365-384.
- (10) Connett, J. M., Anderson, C. J., Baumann, M. L., Schwarz, S. W., Zinn, K. R., Philpott, G. W., and Welch, M. J. (1993) Cu-67 and Cu-64 labeled monoclonal antibody (MAb) as potential agents for radioimmunotherapy. *J. Nucl. Med.* 34, 216P.
- (11) Anderson, C. J., Connett, J. M., Guo, L. W., Schwarz, S. W., Philpott, G. W., Zinn, K. R., and Welch, M. J. (1994) Initial comparison of Cu-67 and Cu-64-labeled anticancer

- carcinoma MAb 1A3 as agents for radioimmunotherapy in tumor-bearing hamsters. *J. Nucl. Med.* 35, 161P.
- (12) Deshpande, S. V., Subramanian, R., McCall, M. J., DeNardo, S. J., DeNardo, G. L., and Meares, C. F. (1990) Metabolism of Indium Chelates Attached to Monoclonal Antibody: Minimal Transchelation of Indium from Benzyl-EDTA Chelate In Vivo. *J. Nucl. Med.* 31, 218–224.
- (13) Deshpande, S. V., DeNardo, S. J., Kukis, D. L., Moi, M. K., McCall, M. J., DeNardo, G. L., and Meares, C. F. (1990) Yttrium-90-Labeled Monoclonal Antibody for Therapy: Labeling by a New Macrocyclic Bifunctional Chelating Agent. *J. Nucl. Med.* 31, 473–479.
- (14) DeNardo, G. L., Kroger, L. A., DeNardo, S. J., Miers, L. A., Salako, Q., Kukis, D. L., Fand, I., Shen, S., Renn, O., and Meares, C. F. (1994) Comparative Toxicity Studies of Yttrium-90 MX-DTPA and 2-IT-BAD Conjugated Monoclonal Antibody (BrE-3). *Cancer* 73, 1012–1022.
- (15) Anderson, C. J., Rogers, B. E., Connett, J. M., Guo, L. W., Schwarz, S. W., Zinn, K. R., and Welch, M. J. (1994) Comparison of Two Bifunctional Chelates for Labeling Cu-64 to MAb 1A3 and 1A3-F(ab)<sub>2</sub>: Chemistry and Animal Biodistribution. *J. Labelled Compd Radiopharm.* 35, 313–315.
- (16) Anderson, C. J., Connett, J. M., Schwarz, S. W., Rocque, P. A., Guo, L. W., Philpott, G. W., Zinn, K. R., Meares, C. F., and Welch, M. J. (1992) Copper-64-Labeled Antibodies for PET Imaging. *J. Nucl. Med.* 33, 1685–1691.
- (17) Anderson, C. J., Schwarz, S. W., Connett, J. M., Cutler, P. D., Guo, L. W., Germain, C. J., Philpott, G. W., Zinn, K. R., Greiner, D. P., Meares, C. F., and Welch, M. J. (1995) Preparation, Biodistribution, and Dosimetry of Copper-64-Labeled Anti-Colorectal Carcinoma Monoclonal Antibody Fragments 1A3-F(ab)<sub>2</sub>. *J. Nucl. Med.* 36, 850–858.
- (18) Subramanian, R., and Meares, C. F. (1990) Bifunctional chelating agents for radiometal-labeled monoclonal antibodies. *Cancer Imaging with Radiolabeled Antibodies* (D. M. Goldenberg, Ed.) pp 183–199, Kluwer Academic Publishers, New York.
- (19) McCall, M. J., Diril, H., and Meares, C. F. (1990) Simplified Method for Conjugating Macrocyclic Bifunctional Chelating Agents to Antibodies via 2-Iminothiolane. *Bioconjugate Chem.* 1, 222–226.
- (20) Smith-Jones, P. M., Fridrich, R., Kaden, T. A., Novak-Hofer, I., Siebold, K., Tschudin, D., and Maecke, H. R. (1991) Antibody Labeling with Copper-67 Using the Bifunctional Macrocyclic 4-[(1,4,8,11-Tetraazacyclotetradec-1-yl)methyl]-benzoic Acid. *Bioconjugate Chem.* 2, 415–421.
- (21) Motekaitis, R. J., Rogers, B. E., Reichert, D. E., Martell, A. E., and Welch, M. J. (1996) Stability and Structure of Activated Macrocyclic Ligands with Biological Applications. *Inorg. Chem.*, in press.
- (22) Clarke, E. T., and Martell, A. E. (1991) Stabilities of the alkaline earth and divalent transition metal complexes of the tetraazamacrocyclic tetraacetic acid ligands. *Inorg. Chim. Acta* 190, 27–36.
- (23) Motta-Hennessy, C., Sharkey, R. M., and Goldenberg, D. M. (1990) Metabolism of Indium-111-Labeled Murine Monoclonal Antibody in Tumor and Normal Tissue of the Athymic Mouse. *J. Nucl. Med.* 31, 1510–1519.
- (24) Jones, P. L., Brown, B. A., and Sands, H. (1990) Uptake and Metabolism of <sup>111</sup>In-labeled Monoclonal Antibody B6.2 by the Rat Liver. *Cancer Res.* 50, 852s–856s.
- (25) Sands, H., and Jones, P. L. (1987) Methods for the Study of the Metabolism of Radiolabeled Monoclonal Antibodies by Liver and Tumor. *J. Nucl. Med.* 28, 390–398.
- (26) Paik, C. H., Sood, V. K., Le, N., Cioloca, L., Carrasquillo, J. A., Reynolds, J. C., Neumann, R. D., and Reba, R. C. (1992) Radiolabeled Products in Rat Liver and Serum after Administration of Antibody-Amide-DTPA-Indium-111. *Nucl. Med. Biol.* 19, 517–522.
- (27) Himmelsbach, M., and Wahl, R. L. (1989) Studies on the Metabolic Fate of <sup>111</sup>In-labeled Antibodies. *Int. J. Radiat. Appl. Instrum., Part B* 16, 839–845.
- (28) Duncan, J. R., and Welch, M. J. (1993) Intracellular Metabolism of Indium-111-DTPA Labeled Receptor Targeted Proteins. *J. Nucl. Med.* 34, 1728–1738.
- (29) Franano, F. N., Edwards, W. B., Welch, M. J., and Duncan, J. R. (1994) Metabolism of Receptor Targeted <sup>111</sup>In-DTPA-Glycoproteins: Identification of <sup>111</sup>In-DTPA-ε-lysine as the Primary Metabolic and Excretory Product. *Nucl. Med. Biol.* 21, 1023–1034.
- (30) Rogers, B. E., Franano, F. N., Duncan, J. R., Edwards, W. B., Anderson, C. J., Connett, J. M., and Welch, M. J. (1995) Identification of Metabolites of In-111-DTPA-Monoclonal Antibodies and Antibody Fragments In Vivo. *Cancer Res.* 55, 5714s–5720s.
- (31) Zinn, K. R., Chaudhuri, T. R., Cheng, T. P., Morris, J. S., and Meyer, W. A. (1994) Production of No-Carrier-Added Cu-64 from Zinc Metal Irradiated under Boron Shielding. *Cancer* 73, 774–778.
- (32) Moi, M. K., Meares, C. F., McCall, M. J., Cole, W. C., and DeNardo, S. J. (1985) Copper Chelates as Probes of Biological Systems: Stable Copper Complexes with a Macrocyclic Bifunctional Chelating Agent. *Anal. Biochem.* 148, 249–253.
- (33) Moran, J. K., Greiner, D. P., and Meares, C. F. (1995) Improved Synthesis of 6-[p-(Bromoacetamido)benzyl]-1,4,8,11-tetraazacyclotetradecane-N,N,N',N''-tetraacetic Acid and Development of a Thin-Layer Assay for Thiol-Reactive Bifunctional Chelating Agents. *Bioconj. Chem.* 6, 296–301.
- (34) McMurry, T. J., Brechbiel, M., Kumar, K., and Gansow, O. A. (1992) Convenient Synthesis of Bifunctional Tetraaza Macrocycles. *Bioconjugate Chem.* 3, 108–117.
- (35) Studer, M., and Kaden, T. A. (1986) One-Step Synthesis of Mono-N-substituted Azamacrocyclics with a Carboxylic Group in the Side-Chain and their Complexes with Cu<sup>2+</sup> and Ni<sup>2+</sup>. *Helv. Chim. Acta* 69, 2081–2086.
- (36) Folch, J. R., Lees, M., and Sloane-Stanley, G. H. (1957) Simple method for the isolation and purification of total lipids from animal tissues. *J. Biol. Chem.* 226, 497–509.
- (37) Goldenberg, D. M., Witte, S., and Elster, K. (1966) GW-39: A New Human Tumor Serially Transplantable in the Golden Hamster. *Transplantation* 4, 760–763.
- (38) Rogers, B. E. (1995) Synthesis and Investigation of Bifunctional Chelating Agents for Radiolabeling Monoclonal Antibodies. Ph.D. Thesis, Washington University.
- (39) Rana, T. M., and Meares, C. F. (1990) N-Terminal Modification of Immunoglobulin Polypeptide Chains Tagged with Isothiocyanato Chelates. *Bioconjugate Chem.* 1, 357–362.
- (40) Means, G. E., and Feeney, R. E. (1971) *Chemical Modification of Proteins*, pp 11–17, Holden-Day, Inc., San Francisco, CA.
- (41) Owen, C. A. (1982) *Biochemical Aspects of Copper: Copper Proteins, Ceruloplasmin, and Copper Protein Binding*, Noyes Publications, New Jersey.
- (42) Winge, D. R. (1984) Normal Physiology of Copper Metabolism. *Semin. Liver Dis.* 4, 239–251.
- (43) Van Hein, P., Kovacs, K., and Matkovic, B. (1975) Properties of Enzymes II. Comparative study of superoxide dismutase activity in rat tissues. *Enzyme* 19, 1–4.
- (44) Meares, C. F., McCall, M. J., Deshpande, S. V., DeNardo, S. J., and Goodwin, D. A. (1988) Chelate Radiochemistry: Cleavable Linkers Lead to Altered Levels of Radioactivity in the Liver. *Int. J. Cancer* 2, 99–102.
- (45) Arano, Y., Mukai, T., Uezono, T., Wakisaka, K., Motonari, H., Akizawa, H., Taoka, Y., and Yokoyama, A. (1994) A Biological Method to Evaluate Bifunctional Chelating Agents to Label Antibodies with Metallic Radionuclides. *J. Nucl. Med.* 35, 890–898.
- (46) Arano, Y., Mukai, T., Akizawa, H., Uezono, T., Motonari, H., Wakisaka, K., Kairiyama, C., and Yokoyama, A. (1995) Radiolabeled Metabolites of Proteins Play a Critical Role in Radioactivity Elimination from the Liver. *Nucl. Med. Biol.* 22, 555–564.
- (47) Anderson, C. J., Pajeau, T. S., Edwards, W. B., Sherman, E. L. C., Rogers, B. E., and Welch, M. J. (1995) In vitro and in vivo Evaluation of Copper-64-Labeled Octreotide Conjugates. *J. Nucl. Med.* 36, 2315–2325.
- (48) Jones-Wilson, T. M. (1995) Preparation and Evaluation of Potential Radiopharmaceuticals labeled with gallium-67,68, indium-111, and Cu-64,67: Relationships between structure and biological activity. Ph.D. Thesis, Washington University.

- (49) Hansch, C., and Leo, A. (1979) *Substituent Constants for Correlation Analysis in Chemistry and Biology*, Wiley-Interscience Publication, New York.
- (50) Maack, T., and Park, C. H. (1990) Endocytosis and lysosomal hydrolysis of proteins in proximal tubules. *Methods Enzymol.* 191, 340–354.
- (51) Martell, A. E., and Smith, R. M. (1982) *Critical Stability Constants*, Plenum Press, New York.
- (52) Kukis, D. L., Li, M., and Meares, C. F. (1993) Selectivity of Antibody-Chelate Conjugates for Binding Copper in the Presence of Competing Metals. *Inorg. Chem.* 32, 3981–3982.
- (53) Maack, T., Park, C. H., and Camargo, J. F. (1992) Renal Filtration, Transport, and Metabolism of Proteins. *The Kidney: Physiology and Pathophysiology* (D. W. Seldin and G. Giebisch, Eds.) pp 3005–3038, Raven Press, Ltd., New York.
- (54) Yokota, T., Milenic, D. E., Whitlow, M., Wood, J. F., Hubert, S. L., and Schlom, J. (1993) Microautoradiographic Analysis of the Normal Organ Distribution of Radioiodinated Single-Chain Fv and Other Immunoglobulin Forms. *Cancer Res.* 53, 3776–3783.
- (55) Fischman, A. J., Pike, M. C., Kroon, D., Fucello, A. J., Rexinger, D., tenKate, C., Wilkinson, R., Rubin, R. H., and Strauss, H. W. (1991) Imaging Focal Sites of Bacterial Infection in Rats with Indium-111-Labeled Chemotactic Peptide Analogs. *J. Nucl. Med.* 32, 483–491.
- (56) Bakker, W. H., Krenning, E. P., Reubi, J. C., Breeman, W. A. P., Setyono-Han, B., de Jong, M., Kooij, P. P. M., Bruns, C., van Hagen, P. M., Marbach, P., Visser, T. J., Pless, J., and Lamberts, S. W. J. (1991) In Vivo Application of [In-111-DTPA-D-Phe]-Octreotide for Detection of Somatostatin Receptor-Positive Tumors in Rats. *Life Sci.* 49, 1593–1601.
- (57) Geissler, F., Anderson, S. K., and Press, O. (1991) Intracellular Catabolism of Radiolabeled Anti-CD3 Antibodies by Leukemic T Cells. *Cell. Immunol.* 137, 96–110.
- (58) Scharschmidt, B. F., Lake, J. R., Renner, E. L., Licko, V., and Van Dyke, R. W. (1986) Fluid phase endocytosis by cultured rat hepatocytes and perfused rat liver: Implications for plasma membrane turnover and vesicular trafficking of fluid phase markers. *Proc. Natl. Acad. Sci. U.S.A.* 83, 9488–9492.
- (59) Yamazaki, K., and LaRusso, N. F. (1989) The Liver and Intracellular Digestion: How Liver Cells Eat! *Hepatology* 10, 877–886.
- (60) Straus, W. (1964) Cytochemical observations on the relationship between lysosomes and phagosomes in the kidney and liver by combined staining for acid phosphatase and intravenously injected horseradish peroxidase. *J. Cell Biol.* 497–507.
- (61) Schneider, Y.-J., Tulkens, P., de Duve, C., and Trouet, A. (1979) Fate of plasma membrane during endocytosis II. Evidence for recycling (shuttle) of plasma membrane constituents. *J. Cell Biol.* 82, 466–474.

BC9600372